Hum Genet (2016) 135:525–540
DOI 10.1007/s00439-016-1660-z

ORIGINAL INVESTIGATION

Expanding the clinical and genetic heterogeneity of hereditary disorders of connective tissue

Anas M. Alazami[1] · Sarah M. Al-Qattan[1] · Eissa Faqeih[2] · Amal Alhashem[3] · Muneera Alshammari[1] · Fatema Alzahrani[1] · Mohammed S. Al-Dosari[1,12] · Nisha Patel[1] · Afaf Alsagheir[4] · Bassam Binabbas[4] · Hamad Alzaidan[9] · Abdulmonem Alsiddiky[5] · Nasser Alharbi[6] · Majid Alfadhel[7] · Amal Kentab[6] · Riza M. Daza[8] · Martin Kircher[8] · Jay Shendure[8] · Mais Hashem[1] · Saif Alshahrani[9] · Zuhair Rahbeeni[9] · Ola Khalifa[9,11] · Ranad Shaheen[1] · Fowzan S. Alkuraya[1,10]

Received: 31 December 2015 / Accepted: 17 March 2016 / Published online: 29 March 2016

Abstract Ehlers–Danlos syndrome (EDS) describes a group of clinical entities in which the connective tissue, primarily that of the skin, joint and vessels, is abnormal, although the resulting clinical manifestations can vary widely between the different historical subtypes. Many cases of hereditary disorders of connective tissue that do not seem to fit these historical subtypes exist. The aim of this study is to describe a large series of patients with inherited connective tissue disorders evaluated by our clinical genetics service and for whom a likely causal variant was identified. In addition to clinical phenotyping, patients underwent various genetic tests including molecular karyotyping, candidate gene analysis, autozygome analysis, and whole-exome and whole-genome sequencing as appropriate. We describe a cohort of 69 individuals representing 40 families, all referred because of suspicion of an inherited connective tissue disorder by their primary physician. Molecular lesions included variants in the previously published disease genes *B3GALT6*, *GORAB*, *ZNF469*, *B3GAT3*, *ALDH18A1*, *FKBP14*, *PYCR1*, *CHST14* and *SPARC* with interesting variations on the published clinical phenotypes. We also describe the first recessive EDS-like condition to be caused by a recessive *COL1A1* variant. In addition, exome capture in a familial case identified a homozygous truncating variant in a novel and compelling candidate gene, *AEBP1*. Finally, we also describe a distinct novel clinical syndrome of cutis laxa and marked facial features and propose *ATP6V1E1* and *ATP6V0D2* (two subunits of vacuolar ATPase) as likely candidate genes based on whole-genome and whole-exome sequencing of the two families with this new clinical entity. Our study expands the clinical spectrum of hereditary disorders of connective tissue and adds three novel candidate genes including two that are associated with a highly distinct syndrome.

Anas M. Alazami and Sarah M. Al-Qattan have contributed equally.

✉ Fowzan S. Alkuraya
falkuraya@kfshrc.edu.sa

1 Department of Genetics, King Faisal Specialist Hospital and Research Center, Riyadh, Saudi Arabia

2 Department of Pediatrics, King Fahad Medical City, Riyadh, Saudi Arabia

3 Department of Pediatrics, Prince Sultan Military Medical City, Riyadh, Saudi Arabia

4 Department of Pediatrics, King Faisal Specialist Hospital and Research Center, Riyadh, Saudi Arabia

5 Department of Orthopedics, College of Medicine, King Saud University, Riyadh, Saudi Arabia

6 Department of Pediatrics, College of Medicine, King Saud University, Riyadh, Saudi Arabia

7 Division of Genetics, Department of Pediatrics, King Abdulaziz Medical City, King Saud Bin Abdulaziz University for Health Sciences, Riyadh, Saudi Arabia

8 Department of Genome Sciences, University of Washington, Seattle, WA, USA

9 Department of Medical Genetics, King Faisal Specialist Hospital and Research Center, Riyadh, Saudi Arabia

10 Department of Anatomy and Cell Biology, College of Medicine, Alfaisal University, Riyadh, Saudi Arabia

11 Department of Pediatrics, Faculty of Medicine, Ain Shams University, Cairo, Egypt

12 Department of Pharmacognosy, College of Pharmacy, King Saud University, Riyadh, Saudi Arabia

Introduction

Ehlers–Danlos syndrome (EDS) is a term that encompasses a wide range of clinical disorders in which defective connective tissue manifests as joint hypermobility and skin and vascular fragility, in addition to a variety of associated clinical features (Beighton 1993; Malfait and De Paepe 2014). Attempts to produce sets of consensus-derived criteria for the broad differential diagnoses that were emerging for individuals presenting with features suggestive of altered connective tissue go back to the Berlin nosology of 1986 (Beighton et al. 1988). The highly variable clinical presentation prompted an effort to classify patients with EDS into more homogeneous groups that can aid in diagnosis and management, and this resulted in the establishment of six major types: classical (Types I, II), hypermobility (Type III), vascular (Type IV), kyphoscoliotic (Type VI), arthrochalasia (Types VIIA, VIIB) and dermatosparaxis (Type VII-C) (Beighton et al. 1998). This classification acknowledges the presence of "others" including "unspecified" forms making it clear that the clinical (and indeed genetic, as subsequently revealed) heterogeneity of EDS could not be fully captured by that classification (De Paepe and Malfait 2012). Indeed, there have been numerous reports of patients with hereditary disorders of connective tissue, who have overlapping clinical manifestations of EDS, but do not meet the diagnostic criteria set forth by the nosology. For decades, the genetic basis of heritable disorders of connective tissue had remained largely unknown. The rise of molecular genetics and its advances in next-generation sequencing unlocked doors that continue to lead to major advances in understanding the molecular pathogenesis of this clinically heterogeneous group of disorders. Nonetheless, much remains to be determined, clinically and molecularly, about these conditions, and little has been published on EDS-like spectrum of phenotypes (Malfait and De Paepe 2014). Furthermore, studies investigating the molecular lesions in hereditary disorders of connective tissue have each almost always described the genetic analysis of one particular condition (Gardeitchik et al. 2014). Thus, there is a need for clinically well-phenotyped cohorts of patients with inherited connective tissue disorders undergoing detailed molecular studies, to provide data that can guide clinical geneticists who are frequently referred such cases. In an attempt to address this, we describe the largest series to date of patients who were all referred with a clinical suspicion of an inherited connective tissue disorder based primarily on joint and skin manifestations. Our comprehensive genomic analysis revealed a striking degree of genetic heterogeneity that enabled us to expand previously established links between genes and certain inherited connective tissue disorder subtypes. In addition, we describe three novel candidate disease genes, two of which appear to underlie an apparently novel and recognizable syndrome.

Subjects and methods

Human subjects

All subjects were referred to the clinical genetics service with the clinical suspicion of an inherited connective tissue disorder because of joint laxity, with or without skin findings in the form of hyperelasticity or excessive wrinkling. Full clinical genetics evaluation was performed on all subjects. Subjects and available family members were enrolled after signing a written informed consent as part of an IRB-approved research protocol (KFSHRC RAC# 2080 006 and 2090 035). Venous blood was collected in EDTA and, as appropriate, in Na-heparin tubes for DNA extraction and establishment of EBV-transformed lymphoblastoid cells, respectively. Those whose clinical photographs are shown have specifically signed a patient photograph release form.

Gene mapping

Determination of the full set of autozygous blocks per genome (autozygome) was as described before (Alkuraya 2012). Briefly, genome-wide genotyping using the Axiom platform was followed by identification of runs of homozygosity >1 Mb as surrogates of autozygosity using AutoSNPa v4. Autozygome was used to either guide candidate gene sequencing by Sanger or to filter the variants generated by whole-exome and whole-genome sequencing. Exome capture was performed using TruSeq Exome Enrichment kit (Illumina) following the manufacturer's protocol. Samples were prepared as an Illumina sequencing library, and in the second step the sequencing libraries were enriched for the desired target using the Illumina Exome Enrichment protocol. The captured libraries were sequenced using Illumina HiSeq 2000 Sequencer. The reads were mapped against UCSC hg19 (http://genome.ucsc.edu/) by BWA (http://bio-bwa.sourceforge.net/). The SNPs and Indels were detected by SAMTOOLS (http://samtools.sourceforge.net/).

For whole genome sequencing, amplification free Illumina TrueSeq libraries were prepared, pooled and then sequenced on six different Illumina HiSeq runs. Full-length paired-end reads were aligned using BWA MEM to Homo sapiens GRCh37 reference sequence (1000 Genomes project phase 2; ftp://ftp.1000genomes.ebi.ac.uk/vol1/ftp/technical/reference/human_g1k_v37.fasta.gz) with default parameters. BWA output was directly BAM converted

and genomic coordinate sorted, then subjected to a GATK insertion/deletion realignment process. We obtained average genome coverage of 12–17×. Variants were called using both GATK's UnifiedGenoTyper 3.2-2 and HaplotypeCaller 3.2-2. Both sets were filtered to remove variants that were present in more than 50 % of individuals, those with less than three reads coverage and those with above 2.5 % minor allele frequency in 1000 Genomes phase 3 release or the Exome Sequencing Project.

For both whole-exome and whole-genome sequencing, the candidacy of the resulting variants was based on their physical location within the autozygome of the affected individual, their population frequency and predicted effect on the protein as described before (Alkuraya 2013) (Figs. 2d, 4c).

Molecular karyotyping

Among the molecular lesions identified in our patients was a de novo 6q24.3-25.2 deletion revealed by molecular karyotyping. The CytoScan HD (Affymetrix) array was used. This array platform contains 2.6 million markers for CNV detection (Affymetrix), of which 750,000 are genotype SNPs and 1.9 million are nonpolymorphic probes, for the whole genome coverage. The analysis was performed using the Chromosome Analysis Suite version Cyto 2.0.0.195(r5758). Oligonucleotide probe information is based on build 37 of the UCSC Genome Browser (http://genome.ucsc.edu/cgi-bin/hgGateway, GRCh37/hg19).

Briefly, 250 ng of genomic DNA was digested with the restriction enzyme NspI and then ligated to an adapter, followed by polymerase chain reaction (PCR) amplification using a single pair of primers that recognized the adapter sequence. The PCR products were run on a 2 % Tris–borate-EDTA (TBE) gel to confirm that the majority of products were between 150 and 2000 bp in length. To obtain a sufficient quantity of PCR product for further analysis, all products from each sample were combined and purified using magnetic beads (Agencourt AMPure, Beckman Coulter, Beverly, MA, USA). The purified PCR products were fragmented using DNase I and visualized on a 4 % TBE agarose gel to confirm that the fragment sizes ranged from 25 to 125 bp. The fragmented PCR products were subsequently end labeled with biotin and hybridized to the array. The arrays were then washed and stained using a GeneChip Fluidics Station 450 and scanned using an Affymetrix GeneChip Scanner 3000 7G. Scanned data files were generated using Affymetrix GeneChip Command Console Software (version 1.2) and analyzed with the Chromosome Analysis Suite.

The hidden Markov model available within the Chromosome Analysis Suite software package was used to determine the copy-number states and their break points. Thresholds of log2 ratio ≥ 0.58 and ≤ -1 were used to categorize altered regions as CNV gains (amplification) and copy-number losses (deletions), respectively.

To minimize the detection of false-positive CNVs arising due to inherent microarray "noise," only alterations that involved at least 50 consecutive probes and that were at least 500 kb in size were used to categorize the altered regions as CNV gains (amplification), whereas those at least 200 kb in size were used to categorize copy-number losses (deletions).

We then proceeded to evaluate the CNVs detected in our patient based on the ACMG standards and guidelines. The genic content in the CNV interval was taken into consideration by seeking recent publications to compare break points, phenotypes and different sizes of CNVs that overlapped. To exclude aberrations representing common benign CNVs, all the identified CNVs were compared with those reported in the Database of Genomic Variants (http://projects.tcag.ca/variation/) and in our own database for individuals who have been classified as normal.

De novo CNVs that met the size cutoff of 200 kb for deletions and 500 kb for duplications (based on the laboratory's consideration of the performance characteristics of the assay used) and were not found in either parent were classified as pathogenic. However, this does not eliminate the possibility that pathogenic CNVs exhibiting incomplete penetrance or variable expressivity can be present in an unaffected parent.

Results

Clinical phenotypes

Unpublished cases of inherited connective tissue disorders

Our cohort consists of 69 subjects from 40 families. The majority of these presented with reduced elasticity of the skin coupled with joint hyperlaxity (unlike EDS, where skin elasticity is increased). This combination is indicative of cutis laxa and accounted for >90 % ($n = 66$ subjects representing 37 families) of the study families. Furthermore, of this cutis laxa cohort many (>40 %, $n = 28$ subjects representing 15 families) had a classical geroderma osteodysplasticum (GO) phenotype, which combines cutis laxa with osseous changes including osteoporosis. This recurrent GO phenotype was caused by a previously reported *GORAB* Saudi founder variant detected by autozygosity-guided candidate gene sequencing in the first few families and by targeted variant analysis in the rest (Al-Dosari and Alkuraya 2009). In Family 2, the phenotype was not consistent with GO, and autozygosity-guided candidate gene analysis led to the

identification of a novel variant in *ALDH18A1*, a known cutis laxa disease gene (Bicknell et al. 2008) (Fig. 1:a1–4). On the other hand, Family 10 presented clinically with many of the features of GO including wrinkly skin and osteopenia. However, spondyloepimetaphyseal dysplasia was diagnosed on skeletal survey. Autozygome analysis did not highlight any of the known cutis laxa genes, so we proceeded with whole-exome sequencing, which revealed a novel variant in *B3GAT3*, a gene known to cause the syndrome of "Multiple joint dislocations, short stature, craniofacial dysmorphism, and congenital heart defects" (Baasanjav et al. 2011). Family 11, presenting with cutis laxa and hypermobility along with muscular dystrophy, was assessed through exome and found to contain a missense variant in *CAPN3*, a gene associated with limb girdle muscular dystrophy (Fig. 1: e1, 2). Two affected individuals in Family 34 exhibited severe intrauterine growth retardation in addition to skin and joint laxity and were found to have a truncating variant in *OBSL1*, a gene implicated in 3-M syndrome. A splice site variant in *PRDM5*, a gene that is known to cause brittle cornea syndrome, was found in Family 36 that presented with blue sclera in addition to joint laxity (Fig. 1: m1). Family 37 includes a previously published case of severe de Barsy syndrome in which autozygome-guided candidate gene sequencing revealed a variant in *PYCR1* (Al-Owain et al. 2012a, b).

Family 40 is worth special mention. This girl presented with short stature and a severe form of cutis laxa. Autozygome-guided candidate gene analysis and whole-exome sequencing did not reveal any likely candidate. Because this is a simplex case, we considered the remote possibility of a chromosomal aberration despite the normal cognition and lack of associated congenital malformation. Molecular karyotyping revealed a de novo 6q24.3-25.2 deletion of 6992 kb (hg18, chr6:146352899-153345216) involving many genes (*GRM1*, *RAB32*, *ADGB*, *LOC729176*, *LOC729178*, *STXBP5*, *SAMD5*, *SASH1*, *UST*, *LOC100128176*, *TAB 2*, *SUMO4*, *ZC3H12D*, *PPIL4*, *C6orf72*, *KATNA1*, *LATS1*, *NUP43*, *PCMT1*, *LRP11*, *LOC100652739*, *RAET1E*, *RAET1G*, *ULBP2*, *ULBP1*, *RAET1 K*, *RAET1L*, *ULBP3*, *PPP1R14C*, *IYD*, *PLEKHG1*, *MTHFD1L*, *AKAP12*, *ZBTB2*, *RMND1*, *C6orf211*, *CCDC170*, *ESR1*, *SYNE1*, *MYCT1*, *VIP*, *FBXO5*, *MTRF1L*, *RGS17*). One gene, *UST*, is particularly intriguing since it encodes uronyl-2-sulfotransferase, which sulfates iduronyl and glucuronyl residues in dermatan/chondroitin sulfate, the major components of the connective tissue. Although we could not identify a likely pathogenic allele in trans on exome sequencing, we cannot exclude the possibility of a deep splicing variant that may have caused the phenotype recessively as a function of hemizygosity. These cases and their molecular findings are summarized in Table 1, and the detailed clinical assessment of these patients can be found in Supplementary Table 1.

Fig. 1 Clinical features of patients with confirmed molecular findings in known disease genes. Family 2 (ALDH18A1) (**a1**–**a4**): **a1** Image of index case. **a2** Facial features. **a3** Visible veins of the abdomen. **a4** Skin laxity. Family 7 (B3GALT6) (**b1**, **b2**): **b1** facial features of the index case; **b2** facial features of the affected cousin. Family 8 (B3GALT6): **c1** facial features of the index case. Family 9 (B3GALT6) (**d1**–**d5**): **d1** image of index case showing rhizomelia; **d2** pectus carinatum; **d3** back showing severe kyphoscoliosis; **d4** right hand showing joint laxity; **d5** lower limbs showing bilateral talipes equinovarus. Family 11 (CAPN3) (**e1**, **e2**): **e1** right hand showing joint laxity at the interphalangeal joints; **e2** overriding toes and hypoplasia of the nails. Family 12 (CHST14) (**f1**–**f6**): **f1** facial features of the index case; **f2** profile of the index case; **f3** hands of the index case showing arthrogryposis; **f4** facial features of the affected brother; **f5** profile of the affected brother; **f6** hands of the affected brother showing arthrogryposis. Family 13 (COL1A1) (**g1**–**g4**): **g1** facial features of the index case; **g2** left hand showing joint laxity at the wrist; **g3** wrinkled skin over the abdomen; **g4** joint laxity at the ankles demonstrated by exaggerated dorsiflexion of the right foot. Family 14 (COL1A1) (**h1**–**h3**): **h1** facial features of the index case; **h2** right arm showing joint laxity at the wrist; **h3** wrinkled skin over the abdomen. Family 15 (COL6A2) (**i1**, **i2**): **i1** facial features of the index case; **i2** left hand showing joint laxity at the fifth metacarpophalangeal joint. Family 28 (GORAB) (**j1**–**j3**): **j1** facial features of the index case; **j2** wrinkled skin over the dorsum of the right hand; **j3** deep palmar creases. Family 31 (GORAB) (**k1**–**k3**): **k1** facial feature of the index case; **k2** wrinkled skin over the dorsal aspect of the digits; **k3** deep palmar creases. Family 35 (PLP1) (**l1**–**l3**): **l1** facial features of index case; **l2** right hand showing joint laxity at the third metacarpophalangeal joint; **l3** right foot showing prominent calcaneum. Family 36 (PRDM5) (**m1**): facial features of the index case. Family 40 (de novo 6q24.3-25.2 deletion) (**n1**): right hand showing increased joint laxity at the interphalangeal joint

Family 38 consists of two siblings born to consanguineous Sudanese parents who presented with short stature, severe joint laxity and scoliosis (Fig. 2a–c). The index case presented with progressive scoliosis that started at 2 years of age. Upon examination, his growth parameters revealed short stature, and he was found to be cognitively normal with mild dysmorphic features including short neck, low-set ears and blue sclera. Examination of his mouth revealed a narrow palate, excessive dental caries (brittle teeth) and ulcers on the tongue. Moreover, he was found to have pectus excavatum and laxity of all joints (without subluxation). His skeletal survey reported diminished bone density. His similarly affected 6-year-old sister presented with progressive scoliosis that also started at 2 years of age. Upon examination, she was also cognitively normal with short stature, joint laxity (without subluxation) and mild dysmorphic features including short neck, low-set ears and blue sclera with a narrow palate, excessive dental caries (brittle teeth) and ulcers on the tongue. Whole-exome sequencing data were filtered according to our pipeline (Fig. 2d) and revealed a single surviving variant, a homozygous splice site alteration immediately downstream of exon 2

in *SPARC* (Fig. 2e). This gene, which encodes a cysteine-rich matrix-associated protein, was not associated with any disease at the time of our exome sequencing, but has since been implicated in osteogenesis imperfecta (Mendoza-Londono et al. 2015). Two patients, both harboring missense variants, have been published presenting with severe bone fragility, progressive scoliosis and joint hyperlaxity. Teeth were indicated as normal. Our patients, who are predicted to have null expression of the protein due to exclusion of the initiation codon-containing exon 2 (Fig. 2f), have in addition blue sclera and brittle teeth, and this may be due to the difference in the nature of the genetic variants.

Other previously reported inherited connective tissue disorder phenotypes

Family 39 is a previously reported family of five children affected with brittle cornea and significant musculoskeletal findings primarily in the form of joint hypermobility

Fig. 1 continued

and severe kyphoscoliosis (Al-Owain et al. 2012a, b). The underlying variant was determined by autozygome-guided candidate gene sequencing of *ZNF469*.

Families 13 and 14 belong to the same tribe and had a strikingly similar phenotype consisting of distinctive facial appearance, joint laxity and recurrent fracture. The index of Family 13 was referred at 6 months of age with severe joint laxity and hypotonia. He was noted to have brachycephaly, a high forehead, blue sclera, mid-face hypoplasia, saggy cheeks and microstomia. He also had wrinkled skin over the abdomen and dorsum of the hands and feet (Fig. 1: g1–4). The index of Family 14 was referred at 7 months of age as a case of craniofacial dysmorphism, cleft palate, severe hypotonia, joint hypermobility and kyphoscoliosis. She was noted to have a high forehead, blue sclera, mid-face hypoplasia, saggy cheeks, and microstomia. In addition to Mongolian spots, she had wrinkled skin over the abdomen, as well as the dorsum of her hands and feet (Fig. 1: h1–3). The skeletal survey showed generalized osteopenia, subluxation of the hip joint with coxa vara and s-shaped scoliosis.

Table 1 Summary of clinical and molecular findings in our EDS-like cohort

Family ID	Phenotype	Gene	Mutation
Family 1 ID: 14DG1601 (2 affected individuals)	Severe skin and joint laxity with dislocations of the hips, knees and ankles, severe osteopenia and Klippel–Feil anomaly, facial dysmorphism (low posterior hairline, bilateral ptosis, sagged face (with soft redundant skin), large ears, a narrow palate, abnormal dental alignment and webbed neck)	AEBP1	NM_001129.3: c.1630+1G>A Homozygous
Family 2 ID: 12DG1019	Cutis laxa, visible veins, sparse hair and facial dysmorphism (progeroid appearance, prominent forehead, midface hypoplasia, prominent mandible, an upturned nose with hypoplastic alae nasi and large low-set ears) cataract, laryngomalacia, seizure disorder, severe global developmental delay, hypotonia, feeding difficulties and poor postnatal growth, scoliosis, inguinal hernia, out-turned lower extremities, TEV and ASD secundum	ALDH18A1	NM_002860.3: c.332A>G (p.E111G) Homozygous
Family 3 ID: 13DG0900	Skin and joint laxity, facial dysmorphism (triangular face, congenital cataract, hypertelorism, short nose, low-set ears, long philtrum, and small chin), Wormian bones, camptodactyly of the thumbs, genu valgum, and VSD	ALDH18A1	NM_001017423: c.251G>A (p.R84Q) Homozygous
Family 4 ID: 13DG1420	Skin and joint laxity, global developmental delay, dysmorphic features (triangular face, upslanting palpebral fissures, severe hooding of the eyelids, depressed nasal bridge, bulbous nose, upturned nostrils and downturned corners of the mouth), borderline microcephaly, underweight, undescended testes and CDH	ATP6V0D2	NM_152565: c.476C>T (p.P159L) Homozygous
Family 5 ID: 10DG0257 (2 affected individuals)	Cutis laxa, dysmorphic features (short forehead, shallow furrowing at forehead midline, blepharophimosis, strabismus, entropion, infraorbital puffiness, maxillary hypoplasia, crowding of the teeth, prominent jaw, saggy cheeks, an abnormal bulge of the upper third of the nasal spine, saddle nose, anteverted nares (almost tented tip of the nose), long philtrum, midline cleft palate, microstomia), nephrocalcinosis and congenital heart defects	ATP6V1E1	NM_001696.3: c.634C>T (p.R212 W) Homozygous
Family 6 ID: 12DG0715	Severe skin and joint laxity, history of multiple fractures, blue sclera with no facial dysmorphism, severe khyphoscoliosis, marked acetabular dysplasia, bilateral radial head dislocation, developmental delay and severe short stature	B3GALT6	NM_080605.3: c.556T>C (p.F186L) Homozygous
Family 7 ID: 12DG1291 (2 affected individuals)	Severe skin and joint laxity with multiple dislocations of both small and large joints, fractures, blue sclera, facial dysmorphism, kyphoscoliosis, TEV, hypotonia, motor delay and cognitive impairment with brain atrophy	B3GALT6	NM_080605.3: c.556T>C (p.F186L) Homozygous

Table 1 continued

Family ID	Phenotype	Gene	Mutation
Family 8 ID: 12DG2397	Joint laxity, multiple joint dislocations, distal arthrogryposis, arachnodactyly, AS, dysmorphic features (broad prominent forehead, arched eyebrows, long eyelashes, deep-set eyes, mildly depressed nasal bridge with upturned nostrils, smooth lips, low-set ears and a short neck with a low hairline)	B3GALT6	NM_080605.3: c.556T>C (p.F186L) Homozygous
Family 9 ID: 12DG2007	Spondyloepimetaphyseal dysplasia, rhizomelia, multiple joint dislocations of the elbows and knees, profound joint hyperlaxity, bilateral TEV, severe progressive kyphoscoliosis, relative macrocephaly, short stature, global developmental delay, dysmorphism (blue sclera, downstlanting palpebral fissures, depressed nasal bridge and upturned nares), MVP, middle ear effusion and asthma GERD	B3GALT6	NM_080605.3: c.536_541dupGCCGCC, (p.R179_R180dup) Homozygous
Family 10 ID: 10DG1458	Spondyloepimetaphyseal dysplasia, cutis laxa, osteoporosis, fracture, multiple bony chondromas and short stature	B3GAT3	NM_012200: c.245C>T (p.P82L) Homozygous
Family 11 ID: 12DG1367	Cutis laxa, hand joint hypermobility, CDH, muscular dystrophy, ID, hypotonia, strabismus, very mild nystagmus, MVP, ASD secundum, dysmorphic features (flat occiput, broad nasal bridge, narrowing of the nose, deep groove of nasolabial fold of ala nasi, very short/underdeveloped columella, narrow palate, crowded teeth and pointed chin), scoliosis, overriding toes, hypoplasia of the nails and flat foot	CAPN3	NM_173087: c.1325G>A (p.R442Q) Homozygous
Family 12 ID: 10DG0445 (2 affected individuals)	Skin and joint laxity, developmental delay, failure to thrive, short stature, dysmorphic features (wide forehead, severe malar hypoplasia, and saggy cheeks), strabismus, decreased hearing, easy bruising, scoliosis, bilateral TEV, arthrogryposis and decreased bone density	CHST14	NM_130468.3: c.48_72del (p.G19Wfs*19) Homozygous
Family 13 ID: 5090066	Skin and joint laxity, respiratory distress at birth, craniofacial dysmorphism (high forehead, blue sclera, mid-face hypoplasia, saggy cheeks, and microstomia/carp mouth), severe hypotonia with muscle wasting, head lag and absent reflexes	COL1A1	NM_000088.3: c.2050G>A (p.Glu684Lys) Homozygous
Family 14 ID: 5095065	Skin and joint laxity, respiratory distress at birth, craniofacial dysmorphism (high forehead, blue sclera, mid-face hypoplasia, saggy cheeks and microstomia/carp mouth), severe hypotonia with muscle wasting, head lag and absent reflexes	COL1A1	NM_000088.3: c.2050G>A (p.Glu684Lys) Homozygous

Table 1 continued

Family ID	Phenotype	Gene	Mutation
Family 15 ID: 08DG-00460 (3 affected individuals)	Extreme distal joint laxity, with proximal large joint limitation, gross motor delay with generalized hypotonia, CDH, microcephaly and failure to thrive	COL6A2	NM_001849.3: c.1459-63G>A Homozygous
Family 16 ID: 08DG-00138 (2 affected individuals)	Significant skin and joint laxity, developmental delay, failure to thrive, severe proportionate short stature with relative macrocephaly, dysmorphic features (prominent forehead, hypoplastic midface, depressed nasal root, anteverted nares and full lips), hyperlordosis, thin slender long tubular bones, small pelvises with winged iliac bones and prominent heels	CUL7	NM_001168370: c.1144C>T (p.R382*) Homozygous
Family 17 ID: 07DG-0027	Significant skin and joint laxity, excessively redundant umbilical skin, hypotonia, myopathy, global developmental delay, microcephaly, subtle dysmorphic features (sloping forehead, square nasal root, mild hypotelorism and epicanthal folds), and PDA	FKBP14	NM_017946.3: c.197+5_197 + 8delGTAA Homozygous
Family 18 ID: 08-00017 (2 affected individuals)	Skin and joint laxity, osteoporosis, good physical growth with typical gerodermia osteodysplastica facies (demonstrated by a senile appearance caused by saggy cheeks and maxillary hypoplasia that gives the impression of prognathism)	GORAB	NM_152281.2: c.306dupA (p.P103Tfs*20) Homozygous
Family 19 ID: 08DG-00103 (2 affected individuals)	Skin and joint laxity, bilateral CDH and flat feet, significant osteopenia, hypotonia, dysmorphic features (progeroid face with decreased infraorbital fatty tissue, a beaked nose and short philtrum)	GORAB	NM_152281.2: c.306dupA (p.P103Tfs*20) Homozygous
Family 20 ID: 08DG-00180 (2 affected individuals)	Skin and joint laxity, right CDH, severe osteopenia, short stature, and dysmorphic features (saggy cheeks, long philtrum, and crowding of the teeth)	GORAB	NM_152281.2: c.306dupA (p.P103Tfs*20) Homozygous
Family 21 ID: 10DG2175	Joint laxity, CDH, osteopenia, fractures, Wormian bones, dysmorphic features (progeroid face with maxillary hypoplasia and mandibular prognathism)	GORAB	NM_152281.2: c.306dupA (p.P103Tfs*20) Homozygous
Family 22 ID: 10DG2176 (4 affected individuals)	Skin and joint laxity, CDH, osteopenia, fractures, Wormian bones, dysmorphic features (progeroid face with maxillary hypoplasia and mandibular prognathism)	GORAB	NM_152281.2: c.306dupA (p.P103Tfs*20) Homozygous
Family 23 ID: 11DG0067	Skin and joint laxity, CDH, osteopenia, fractures, Wormian bones and dysmorphic features (progeroid face with maxillary hypoplasia and mandibular prognathism)	GORAB	NM_152281.2: c.306dupA (p.P103Tfs*20) Homozygous
Family 24 ID: 11DG0213 (3 affected individuals)	Skin and joint laxity, CDH, osteopenia, fractures, Wormian bones and dysmorphic features (progeroid face with maxillary hypoplasia and mandibular prognathism)	GORAB	NM_152281.2: c.306dupA (p.P103Tfs*20) Homozygous
Family 25 ID: 12DG1561	Reduced skin elasticity with excessive wrinkling especially in the abdomen, joint laxity, CDH, motor delay, dysmorphic features (saggy cheeks, over folded upper pinnae)	GORAB	NM_152281.2: c.306dupA (p.P103Tfs*20) Homozygous

Table 1 continued

Family ID	Phenotype	Gene	Mutation
Family 26 ID: 13DG0087	Skin and joint laxity, CDH, scoliosis, fractures, dysmorphic features (sagging face, malar hypoplasia and mandibular prognathism), morbid obesity, linear scleroderma, irregular periods, infertility and depression	GORAB	NM_152281.2: c.306dupA (p.P103Tfs*20) Homozygous
Family 27 ID: DG07-0016 (2 affected individuals)	Skin and joint laxity, CDH, kyphoscoliosis, osteoporosis, fractures, dysmorphic features (senile appearance caused by droopy cheeks, prognathism and malar hypoplasia with significant crowding of maxillary teeth, aplastic lingual frenulum and prominent anteverted ears)	GORAB	NM_152281.2: c.733G>C (p.A245P) Homozygous
Family 28 ID: 10DG2136 (2 affected individuals)	Skin and joint laxity, CDH, bilateral TEV, osteopenia, fractures and dysmorphic features (progeroid face with maxillary hypoplasia) and subaortic stenosis	GORAB	NM_152281.2: c.301_302insA (p.P103Tfs18*) Homozygous
Family 29 ID: 10DG2137	Skin and joint laxity, CDH, osteopenia, fractures, Wormian bones and dysmorphic features (progeroid face with maxillary hypoplasia, and mandibular prognathism)	GORAB	NM_152281.2: c.301_302insA (p.P103Tfs18*) Homozygous
Family 30 ID: 10DG2138 (4 affected individuals)	Skin and joint laxity, CDH, thin bones, fractures, osteopenia, osteoporosis, Wormian bones, low vitamin D, bronchial asthma and dysmorphic features (progeroid faces with maxillary hypoplasia and mandibular prognathism)	GORAB	NM_152281.2: c.301_302insA (p.P103Tfs18*) Homozygous
Family 31 ID: 10DG2141	Skin and joint laxity, CDH, osteoporosis, thin bones and dysmorphic features (droopy face, maxillary hypoplasia and mandibular prognathism)	GORAB	NM_152281.2: c.301_302insA (p.P103Tfs18*) Homozygous
Family 32 ID: 10DG2142	Skin laxity, fractures, osteopenia, Wormian bones and dysmorphic features (progeroid face with maxillary hypoplasia and mandibular prognathism)	GORAB	NM_152281.2: c.301_302insA (p.P103Tfs18*) Homozygous
Family 33 ID: 11DG0058 (3 affected individuals)	Severe skin and joint laxity, ID, sagittal craniosynostosis (dolichocephaly), the typical facial features of CED (prominent forehead, epicanthal folds, depressed nasal bridge, anteverted nares and everted lower lip), micro/hypodontia, short limbs, the typical hand features (brachdactyly, single interphalangeal crease for some fingers and clinodactyly), and narrow thorax	IFT122	NM_052985.2: c.1868G>T (p.G623V) Homozygous
Family 34 ID: 09DG00622 (2 affected individuals)	Skin and joint laxity, severe IUGR, proportionate short stature, and dysmorphic features (triangular face, upswept frontal hair, hypoplastic midface, prominent eyes, low nasal bridge, upturned nose, long philtrum and full lips)	OBSL1	NM_015311.2: c.1306delC (p.R436Gfs*14) Homozygous

Table 1 continued

Family ID	Phenotype	Gene	Mutation
Family 35 ID: 09DG00236 (2 affected individuals)	Severe joint laxity, fractures, global developmental delay, seizure disorder, encephalopathy, severe hypotonia, asthma, subtle dysmorphism (tented upper lip and upturned nose), horizontal nystagmus and exaggerated lordosis	PLP1	NM_000533: c.650G>A (p.G217D) Hemizygous
Family 36 ID: 10DG2065	Marked joint laxity, blue sclera, depressed nasal bridge and mild generalized hypotonia	PRDM5	NM_018699.2: c.343 + 2T > C Homozygous
Family 37 ID: 11DG1872	Pre- and postnatal growth retardation, developmental delay, dysmorphic features (progeroid appearance, large anterior fontanel, widely separated sutures, dilated skull veins with fine sparse hair, prominent forehead, large protruding low-set ears, depressed nasal bridge with pinched nose, thin upper lip vermilion and micrognathia), eye abnormalities (buphthalmos with corneal clouding, glaucoma, bilateral anterior polar cataract), skin abnormalities (thin, lax, wrinkled and translucent with prominent superficial veins giving a reticular pattern), adducted thumbs with overlapping fingers bilaterally, flexion deformities of the elbows and left knee, bilateral talipes calcaneovalgus, history of seizures, atrophic appearance of the corpus callosum, mild gastroesophageal reflux, recurrent chest infections, patent foramen ovale, bilateral renal tubular ectasia, with horseshoe kidneys, dislocation of both hip joints and hypertrophied clitoris	PYCR1	NM_153824.1: c.616G>A (p.G206R) Homozygous
Family 38 ID: 12DG2243 (2 affected individuals)	Marked joint laxity, progressive scoliosis, short stature, normal cognition with mild dysmorphic features (short neck, low-set ears and blue sclera, a narrow palate, excessive dental caries (easily broken teeth) and ulcers on the tongue) and pectus excavatum	SPARC	NM_003118.3: c.57+1G>C Homozygous
Family 39 ID: 10DG1309 (5 affected individuals)	Blue sclera, corneal fragility, joint hypermobility, severe kyphoscoliosis (some requiring spinal fusion surgery), positive Steinberg thumb sign, arachnodactyly, hallux valgus, sensorineural hearing loss, thin velvety skin, (phenylketonuria in one of the siblings who had the mildest ocular and skeletal symptoms in the group)	ZNF469	NM_001127464: c.8817_8830dup (p.E2944Gfs*50) Homozygous
Family 40 ID: DG08RC0005C	Skin and joint laxity, short stature, obesity, dysmorphic features (hooded eyelids, tubular nose and elongated facies), MR, TR and hydronephrosis	De novo 6q24.3-q25.2 deletion	(146,352,899–153,345,216)

AS aortic stenosis, *ASD* atrial septal defect, *CDH* congenital dislocation of the hip, *CED* cranioectodermal dysplasia, *GERD* gastroesophageal reflux disease, *ID* intellectual disability, *IUGR* intrauterine growth restriction, *MR* mitral regurgitation, *MVP* mitral valve prolapse, *PDA* patent ductus arteriosus, *TEV* talipes equinovarus, *TR* tricuspid regurgitation, *VSD* ventricular septal defect

Exome sequencing performed by a clinical laboratory on probands from Families 13 and 14 revealed the same novel homozygous missense variant in *COL1A1* (c.2050G>A, p.Glu684Lys). Although dominant variants in *COL1A1* and *COL1A2* are known to cause EDS phenotypes, this is the first time *COL1A1* is shown to cause EDS in a recessive fashion (parents in both families were completely normal clinically) (Malfait and De Paepe 2014).

Family 33, containing several affected siblings who were originally diagnosed as sagittal craniosynostosis, but also possessed severe skin and joint laxity, and typical craniectodermal dysplasia facial features. Whole-exome sequencing revealed a novel variant in the ciliary gene *IFT122*, and primary cilia exhibited reduced frequency and length in patient fibroblasts (Alazami et al. 2014).

Family 17 was previously reported and was found to have a homozygous truncating variant in *FKBP14* (Aldeeri et al. 2014), which had not been reported as a disease gene at the time of our whole-exome sequencing. Family 12 consists of two siblings who presented with the unusual combination of arthrogryposis, joint laxity and strabismus (Fig. 1: f1–6), and although *CHST14*, a known EDS-like disease gene (Miyake et al. 2010), was clearly within the shared autozygome of the two individuals, it was missed as a good candidate and subsequent whole-exome sequencing revealed a novel homozygous truncating variant. Finally, we have observed a variable phenotype associated with variants in *B3GALT6* (Malfait et al. 2013; Nakajima et al. 2013). Family 9 consisted of consanguineous parents and one affected daughter with profound joint laxity and severe kyphoscoliosis (Fig. 1: d1–5). Skeletal survey revealed spondyloepimetaphyseal dysplasia. Autozygome-guided candidate gene sequencing revealed a novel homozygous truncating variant in *B3GALT6*. On the other hand, we report three families with a founder missense variant in *B3GALT6* that had a variable phenotype. The index in Family 8 presented as an infant with hip dislocation, joint laxity and arthrogryposis (Fig. 1: c1). However, the probands in Family 6 and Family 7 (Fig. 1: b1, 2) presented with severe joint laxity, blue sclera, multiple joint dislocation and recurrent fractures with severe osteopenia reminiscent of osteogenesis imperfecta. The atypical presentation of the probands in the three families precluded the identification of *B3GALT6* as a good candidate in the autozygome-guided candidate gene analysis stage, so they all underwent whole-exome sequencing which revealed the same founder variant.

Of note, our cohort included three clinical entities that are not typically considered as part of the hereditary disorders of connective tissue spectrum, but highlight the extreme heterogeneity of referrals with that diagnosis. Family 16 consists of two siblings with marked joint laxity and short stature. However, their facial features were typical of 3M syndrome and were subsequently found to have *CUL7* variant as previously described (Al-Dosari et al. 2012). Family 15 consists of the index and two cousins who presented with microcephaly, global developmental delay and profound small joint laxity typical of Ullrich muscular dystrophy (Fig. 1: i1, 2). Muscle biopsy confirmed lack of staining for collagen 6 and Sanger sequencing of *COL6A2* revealed a novel deep intronic variant that fully segregated with the phenotype. Lastly, the two brothers in Family 35 presented with severe joint laxity and global developmental delay, but their brain MRI revealed typical white matter changes of Pelizaeus–Merzbacher disease and subsequent sequencing of *PLP1* revealed a novel truncating variant (Fig. 1: l1–3). These cases and their molecular findings are summarized in Table 1, and the detailed clinical assessment of these patients can be found in Supplementary Table 1.

Novel candidate genes for inherited connective tissue disorders

Three families in our cohort did not map to any known disease gene in the context of EDS phenotype and their whole-exome/whole genome sequencing revealed novel candidate genes as follows:

Family 1 consists of two siblings born to first cousin parents (Fig. 3c). They both presented similarly with severe joint and skin laxity, bilateral ptosis, severe osteopenia, webbed neck with low posterior hair line and facial dysmorphism comprising sagged cheeks, large ears, soft and redundant skin, narrow palate, abnormal dental alignment and dislocated hips, knees and ankles (Fig. 3a, b). Clinical whole-exome sequencing revealed only a single variant of interest, a homozygous splicing variant located downstream of exon 13 in *AEBP1* (Fig. 3d), which encodes a member of the carboxypeptidase A protein family. RTPCR revealed loss of the last 22 bp of exon 13, resulting in frameshift and subsequent truncation (Fig. 3e, f).

Family 5 consists of two brothers born to first cousin parents (Fig. 4b). Both had a nearly identical phenotype, which to our knowledge is novel and highly distinct. Pregnancy was complicated by the findings of oligohydramnios, congenital heart disease and hydronephrosis. Apgar scores and growth parameters at birth were normal, but gross dysmorphism was apparent at birth including entropion requiring surgical correction with only partial improvement. As neonates, they were found to have small PFO, small PDA, mild TR and increased pulmonary pressure. They both had hydronephrosis and evidence of nephrocalcionsis. They both have good physical growth and nearly identical dysmorphic profile consisting of wrinkly skin, blepharophimosis, entropion, hypertelorism, malar hypoplasia and severe microstomia (Fig. 4a). Whole-exome sequencing of both siblings was performed,

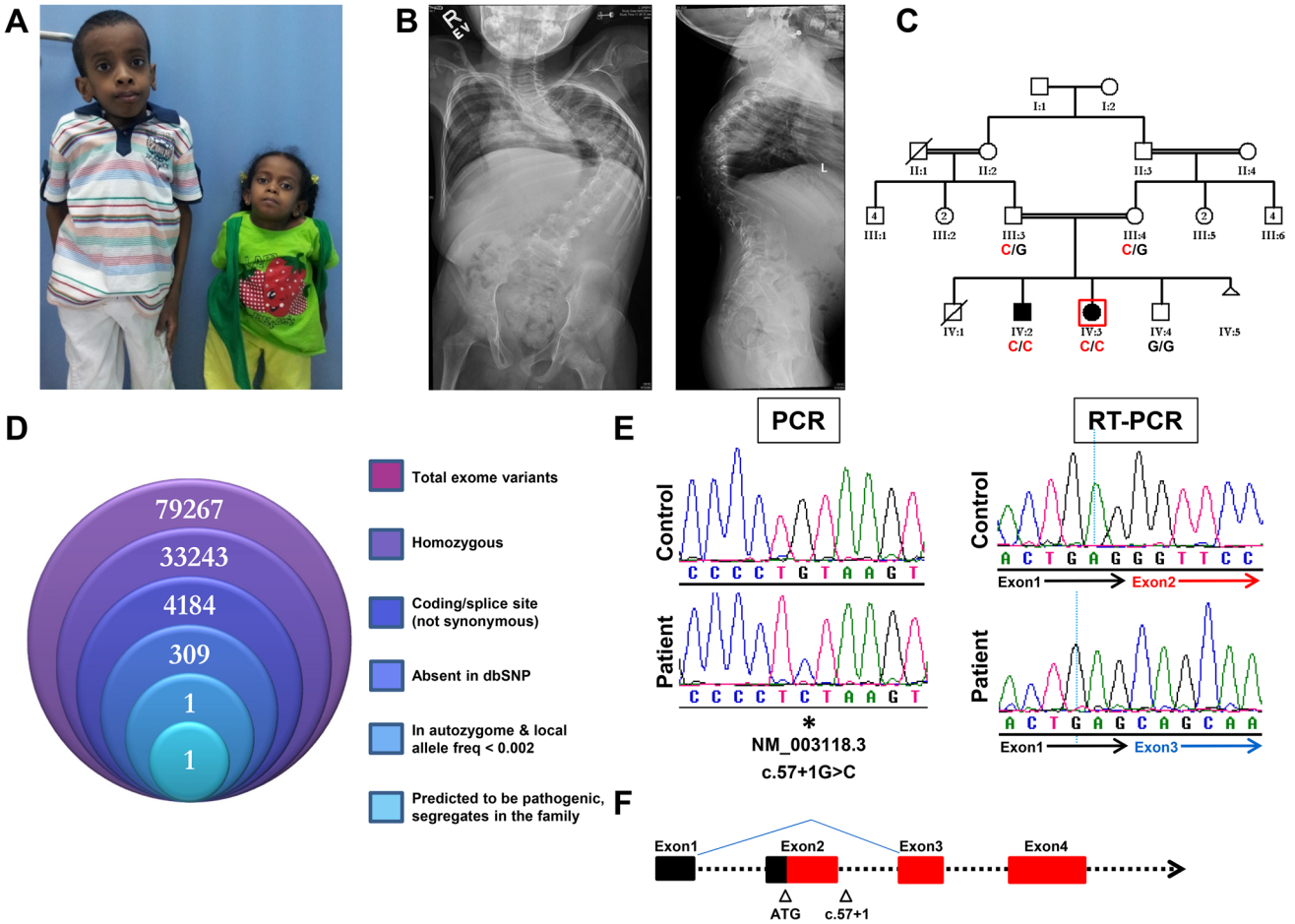

Fig. 2 Family 38: loss of function mutation in *SPARC* causes severe joint laxity and scoliosis; **a** images of the affected siblings; **b** radiology of the older affected, showing severe kyphoscoliotic deformity of thoracolumbar spine with gibbus formation; **c** family pedigree with the genotypes indicated beneath the individuals who were tested; the proband is boxed in *red*. **d** Filtering scheme used in assessing the exome capture data. **e** PCR chromatograph for the patient, along with RT-PCR results that reveal skipping of exon 2. A schematic of the mutation is provided in **f**, with the *blue lines* indicating the skipped exon. Untranslated regions are in *black*, and translated regions in *red*

but did not reveal a good candidate. We therefore proceeded with whole-genome sequencing and filtered the surviving variants according to the pipeline in Fig. 4c. Only a single variant remained, a novel missense variant in a component of vacuolar ATPase, *ATP6V1E1* (Fig. 4d). This variant was missed by both exomes due to coverage issues. The affected residue in *ATP6V1E1* lies in a stretch of amino acids that is universally conserved among mammals (Fig. 4e).

Subsequently, in Family 4, we identified a simplex case born to first cousin parents, whose presentation nearly mirrored that of the above family (Fig. 4f, g). Although exome capture resulted in five variants that survived our filtering (Fig. 4h), we were intrigued to find that one of these was in another component of vacuolar ATPase, *ATP6V0D2*, affecting a residue that is very highly conserved in mammals (Fig. 4i). The full list of identified variants in this case include *ATP6V0D2* (NM_152565: c.476C>T:p.P159L), *MYOM3* (NM_152372: c.554T>C:p.V185A), *ZBTB8OS* (NM_178547: c.166G>A:p.A56T), *TRAPPC12* (NM_016030: c.496C>A:p.R166S), and *BAX* (NM_138763: c.347T>C:p.F116S). These cases and their molecular findings are summarized in Table 1, the detailed clinical assessments of these patients can be found in Supplementary Table 1.

Discussion

Although inherited connective tissue disorder presentations are a common cause of referral to clinical genetics, we are not aware of any clinical report comprising all patients with this presentation. Such cohorts are especially needed in view of the extreme clinical heterogeneity of this group

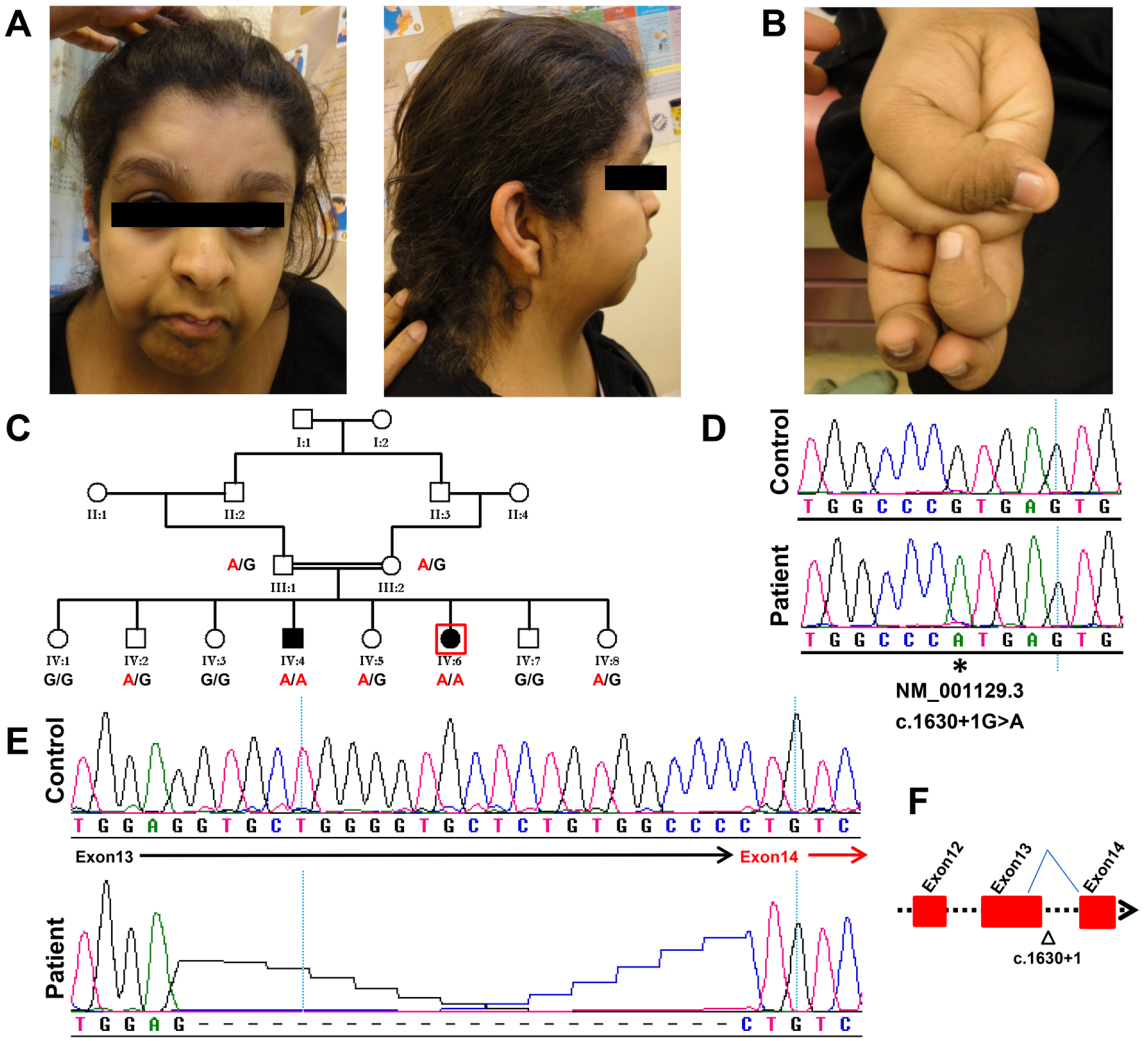

Fig. 3 Family 1: Frameshift mutation in *AEBP1* causes a syndrome of severe joint and skin laxity, severe osteopenia, low posterior hairline and facial dysmorphism. Images of the proband are provided, indicating facial features (**a**) and joint laxity (**b**). **c** Family pedigree with the genotypes listed beneath the individuals who were tested; the proband is boxed in *red*. Chromatographs of the PCR (**d**) and RT-PCR (**e**) data reveal a splice site mutation that results in the skipping of the last 22 bp of exon 13, as illustrated in the schematic (**f**)

of disorders and the recent expansion of genes that have been found to be mutated in these patients (De Paepe and Malfait 2012; Halper 2014; Malfait and De Paepe 2014). The cohort we report in this study represents an attempt to not only capture, but also further expand this heterogeneity. The molecular characterization of our entire cohort gives us a unique opportunity to discuss the clinical phenotype in the context of identified molecular lesions.

We emphasize the highly diverse differential diagnosis of patients with inherited connective tissue disorders. Although EDS and cutis laxa each has a distinct dermatological profile, we note that the clinical distinction may not always be straightforward not only to the referring physician but also to the clinical geneticist. Wrinkly skin, a characteristic finding of cutis laxa, was observed in several of our patients with variants in genes linked previously to inherited connective tissue disorders. Thus, it seems prudent to keep the differential diagnosis open to the possibility of hereditary disorders of connective tissue even in the context of wrinkly skin. Furthermore, our encounter with 3M syndrome, Ullrich muscular dystrophy and Pelizaeus–Merzbacher disease highlights the need for a thorough assessment of patients with inherited connective tissue disorders, which may reveal dysmorphic and neurogenetic disorders not typically considered in the differential diagnosis.

Our comprehensive genomic approach has also allowed us to identify three compelling candidate genes. *AEBP1* encodes adipocyte enhancer binding protein, a secreted protein that binds to the extracellular matrix (Layne et al. 2001). It has a similar embryonic expression pattern as other ECM proteins, including collagens, thrombospondin and decorin (Ith et al. 2005; Layne et al.

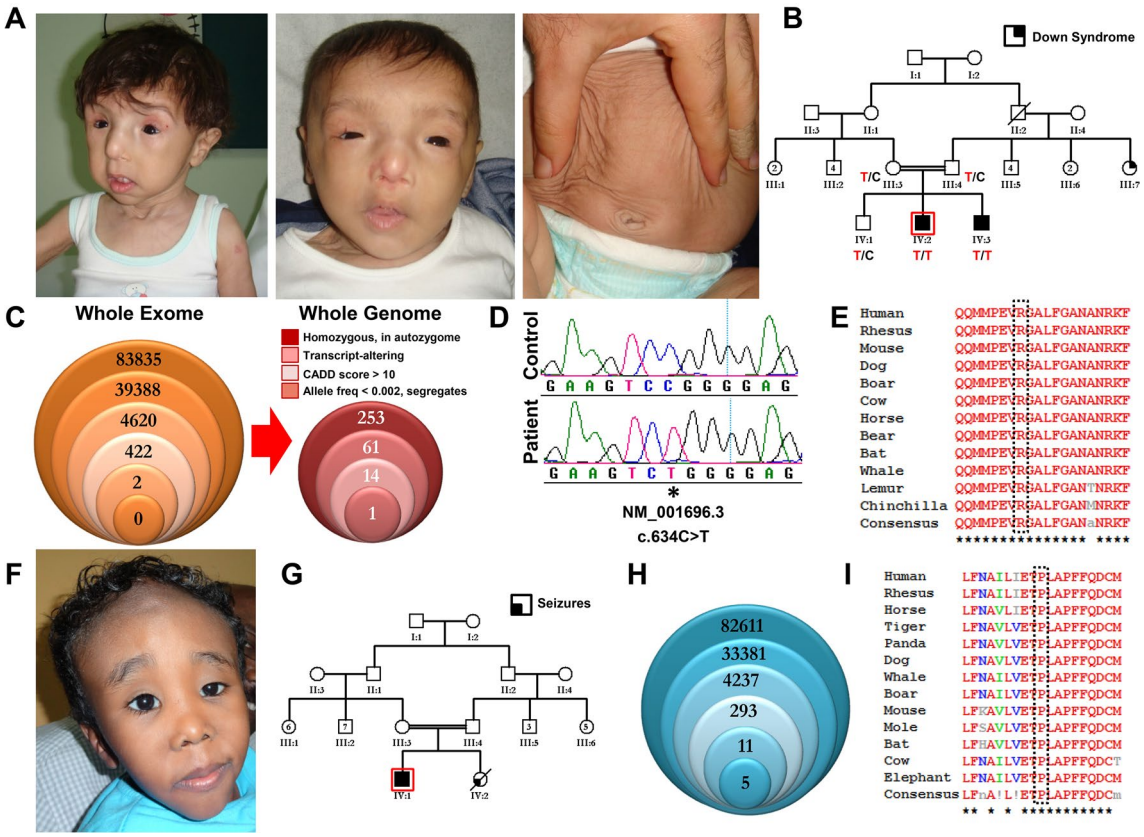

Fig. 4 A unique syndrome of cutis laxa and distinct facies is linked to mutations in the hydrogen-transporting vacuolar ATPase (V-ATPase). **a** Clinical images of both patients from Family 5, along with an associated pedigree (**b**) highlighting the genotypes observed. The proband is boxed in *red*. Exome capture for both sibs failed to reveal any candidates (**c**; only the results for the younger brother are shown, with filtration scheme as given for Fig. 2d. *CADD* combined annotation-dependent depletion). Subsequent whole-genome sequencing data were filtered as indicated. **d** Chromatograph of the *ATP6V1E1* mutation in this family. The affected residue lies in a stretch of amino acids that is universally conserved amongst mammals (**e**). **f** Image of the simplex case of Family 4, along with pedigree (**g**). **h** Results of the filtering scheme for this patient. A total of five variants remain after all filters are applied, including a missense in *ATP6V0D2*. **i** The affected residue in *ATP6V0D2* is very highly conserved among mammals

2001). Interestingly, mice that are knocked out for the long isoform display ventral wall defects and skin that is prone to injuries and has reduced healing capacity (Layne et al. 2001). These features are highly suggestive that the homozygous truncating variant we identified may have caused the phenotype in the two siblings.

The two families with variants in vacuolar ATPase component genes represent an apparently novel and clinically recognizable syndrome consisting of wrinkly skin, entropion and idiopathic nephrocalcinosis. Another subunit of vacuolar ATPase, ATP6V0A2, is known to cause a recognizable form of cutis laxa (Kornak et al. 2008). *ATP6V1E1* is expressed in the developing xenopus skin, but little is known about this gene otherwise (Quigley et al. 2011). We note that the missense variant we identified in this gene fully segregated with the phenotype within the family and is not found in any of the public variant databases including the 1000 Genomes and the ExAC consortium. It is also absent in 573 ethnically matched in-house Saudi exomes. Regarding the simplex case in Family 4, although we were unable to reduce the number of surviving exome capture variants to just one, we note that the missense *ATP6V0D2* variant in our patient may play a role in his nephrocalcinosis given its published role in bone biology (Lee et al. 2006). In addition, the strong phenotypic link between families 4 and 5 and the presence in each family of a variant in a vacuolar ATPase component suggest *ATP6V0D2* as a candidate disease gene for Family 4. However, just as with the other novel candidate gene, a definitive causal link will require the identification of independent pathogenic alleles in other similarly affected patients and we hope our study will be an impetus to screen for variants in these genes by other investigators who have cohorts with overlapping phenotypes.

In conclusion, we report the largest cohort to date on inherited connective tissue disorders referred in a clinical setting for evaluation by clinical genetics. Our results expand the clinical, allelic and locus heterogeneity of these conditions and highlight the need for thorough clinical and genomic evaluation, which are likely to have a high yield in this patient population.

Acknowledgments We thank the families for their enthusiastic participation. We also thank the Genotyping and Sequencing Core Facilities at KFSHRC for their technical help. This work was supported in part by King Salman Center for Disability Research Grant (FSA).

Compliance with ethical standards

Conflict of interest The authors declare no conflict of interest.

References

Alazami AM, Seidahmed MZ, Alzahrani F, Mohammed AO, Alkuraya FS (2014) Novel IFT122 mutation associated with impaired ciliogenesis and cranioectodermal dysplasia. Mol Genet Genom Med 2:103–106

Aldeeri AA, Alazami AM, Hijazi H, Alzahrani F, Alkuraya FS (2014) Excessively redundant umbilical skin as a potential early clinical feature of Morquio syndrome and FKBP14-related Ehlers–Danlos syndrome. Clin Genet 86:469–472

Al-Dosari M, Alkuraya FS (2009) A novel missense mutation in SCYL1BP1 produces geroderma osteodysplastica phenotype indistinguishable from that caused by nullimorphic mutations. Am J Med Genet Part A 149:2093–2098

Al-Dosari MS, Al-Shammari M, Shaheen R, Faqeih E, AlGhofely MA, Boukai A, Alkuraya FS (2012) 3M syndrome: an easily recognizable yet underdiagnosed cause of proportionate short stature. J Pediatr 161(139–145):e1

Alkuraya FS (2012) Discovery of rare homozygous mutations from studies of consanguineous pedigrees. Curr Protoc Hum Genets 6.12. 1–6.12. 13

Alkuraya FS (2013) The application of next-generation sequencing in the autozygosity mapping of human recessive diseases. Hum Genet 132:1197–1211

Al-Owain M, Al-Dosari MS, Sunker A, Shuaib T, Alkuraya FS (2012a) Identification of a novel ZNF469 mutation in a large family with Ehlers–Danlos phenotype. Gene 511:447–450

Al-Owain M, Alanazi S, Khalifa O, Al-Hemidan A, Al-Ebdi L, Al-Saud B, Alkuraya FS (2012b) A case of de Barsy syndrome with a severe eye phenotype. Am J Med Genet Part A 158:2364–2366

Baasanjav S, Al-Gazali L, Hashiguchi T, Mizumoto S, Fischer B, Horn D, Seelow D, Ali BR, Aziz SA, Langer R (2011) Faulty initiation of proteoglycan synthesis causes cardiac and joint defects. Am J Hum Genet 89:15–27

Beighton P (ed) (1993) McKusick's heritable disorders of connective tissue, 5th edn. Mosby, St. Louis

Beighton P, De Paepe A, Danks D, Finidori G, Gedde-Dahl T, Goodman R, Hall J, Hollister D, Horton W, McKusick V (1988) International nosology of heritable disorders of connective tissue, Berlin, 1986. Am J Med Genet 29:581–594

Beighton P, De Paepe A, Steinmann B, Tsipouras P, Wenstrup RJ (1998) Ehlers–Danlos syndromes: revised nosology. Am J Med Genet 77:31–37

Bicknell LS, Pitt J, Aftimos S, Ramadas R, Maw MA, Robertson SP (2008) A missense mutation in ALDH18A1, encoding Δ1-pyrroline-5-carboxylate synthase (P5CS), causes an autosomal recessive neurocutaneous syndrome. Eur J Hum Genet 16:1176–1186

De Paepe A, Malfait F (2012) The Ehlers–Danlos syndrome, a disorder with many faces. Clin Genet 82:1–11

Gardeitchik T, Mohamed M, Fischer B, Lammens M, Lefeber D, Lace B, Parker M, Kim K-J, Lim BC, Häberle J (2014) Clinical and biochemical features guiding the diagnostics in neurometabolic cutis laxa. Eur J Hum Genet 22:888–895

Halper J (2014) Progress in heritable soft connective tissue diseases. Springer, Berlin

Ith B, Wei J, Yet S-F, Perrella MA, Layne MD (2005) Aortic carboxypeptidase-like protein is expressed in collagen-rich tissues during mouse embryonic development. Gene Expr Patterns 5:533–537

Kornak U, Reynders E, Dimopoulou A, van Reeuwijk J, Fischer B, Rajab A, Budde B, Nürnberg P, Foulquier F, Dobyns WB (2008) Impaired glycosylation and cutis laxa caused by mutations in the vesicular H+-ATPase subunit ATP6V0A2. Nat Genet 40:32–34

Layne MD, Yet S-F, Maemura K, Hsieh C-M, Bernfield M, Perrella MA, Lee M-E (2001) Impaired abdominal wall development and deficient wound healing in mice lacking aortic carboxypeptidase-like protein. Mol Cell Biol 21:5256–5261

Lee S-H, Rho J, Jeong D, Sul J-Y, Kim T, Kim N, Kang J-S, Miyamoto T, Suda T, Lee S-K (2006) v-ATPase V0 subunit d2-deficient mice exhibit impaired osteoclast fusion and increased bone formation. Nat Med 12:1403–1409

Malfait F, De Paepe A (2014) The Ehlers-Danlos syndrome. Progress in heritable soft connective tissue diseases. Springer, Berlin, pp 129–143

Malfait F, Kariminejad A, Van Damme T, Gauche C, Syx D, Merhi-Soussi F, Gulberti S, Symoens S, Vanhauwaert S, Willaert A (2013) Defective initiation of glycosaminoglycan synthesis due to B3GALT6 mutations causes a pleiotropic Ehlers–Danlos-syndrome-like connective tissue disorder. Am J Hum Genet 92:935–945

Mendoza-Londono R, Fahiminiya S, Majewski J, Tétreault M, Nadaf J, Kannu P, Sochett E, Howard A, Stimec J, Dupuis L (2015) Recessive osteogenesis imperfecta caused by missense mutations in SPARC. Am J Hum Genet 96(6):979–985

Miyake N, Kosho T, Mizumoto S, Furuichi T, Hatamochi A, Nagashima Y, Arai E, Takahashi K, Kawamura R, Wakui K (2010) Loss-of-function mutations of CHST14 in a new type of Ehlers–Danlos syndrome. Hum Mutat 31:966–974

Nakajima M, Mizumoto S, Miyake N, Kogawa R, Iida A, Ito H, Kitoh H, Hirayama A, Mitsubuchi H, Miyazaki O (2013) Mutations in B3GALT6, which encodes a glycosaminoglycan linker region enzyme, cause a spectrum of skeletal and connective tissue disorders. Am J Hum Genet 92:927–934

Quigley IK, Stubbs JL, Kintner C (2011) Specification of ion transport cells in the Xenopus larval skin. Development 138:705–714